Journal of Translational Autoimmunity 6 (2023) 100182

Contents lists available at ScienceDirect

Journal of Translational Autoimmunity

journal homepage: www.sciencedirect.com/journal/journal-of-translational-autoimmunity

Apoptotic biliary epithelial cells and gut dysbiosis in the induction of murine primary biliary cholangitis

Yu-Wen Wang [a], Chia-I Lin [a], Hung-Wen Chen [a], Jui-Ching Wu [a,b], Ya-Hui Chuang [a,b,*]

[a] Department of Clinical Laboratory Sciences and Medical Biotechnology, College of Medicine, National Taiwan University, Taipei, Taiwan
[b] Department of Laboratory Medicine, National Taiwan University Hospital, College of Medicine, National Taiwan University, Taipei, Taiwan

ARTICLE INFO

Handling editor: M.E. Gershwin

Keywords:
Autoimmune cholangitis
Apoptosis
Gut microbiota
Xenobiotic
Toll-like receptor

ABSTRACT

Primary biliary cholangitis (PBC) is a female-predominant liver autoimmune disease characterized by the specific immune-mediated destruction of the intrahepatic small bile duct. Although apoptosis of biliary epithelial cells (BECs) and alterations in gut microbiota are observed in patients with PBC, it is still unclear whether these events happen in the early stage and cause the breakdown of tolerance in PBC. In this study, we examined the early events in the loss of tolerance in our well-defined 2-OA-OVA-induced murine autoimmune cholangitis (AIC) model. We report herein that apoptosis of BECs was notable in the early stage of murine AIC. An altered gut microbiota, in particular, an increased percentage of gram-positive *Firmicutes* in AIC mice was also observed. BECs in AIC mice expressed adhesion molecule ICAM-1, cytokines/chemokines TNF-α, CCL2, CXCL9, CXCL10, and toll-like receptor (TLR) 2. Moreover, BECs treated with TLR2 ligand had elevated apoptosis and CXCL10 production. These data collectively suggest a new mechanism of tolerance breakdown in AIC. Altered gut microbiota induces apoptosis of BECs through TLR2 signaling. BECs secrete chemokines to recruit CD8 T cells to damage BECs further.

1. Introduction

Primary biliary cholangitis (PBC) is a female-predominant liver autoimmune disease characterized by specific antimitochondrial antibodies (AMAs) and immune-mediated destruction of the intrahepatic small bile duct. The immunodominant mitochondrial autoantigen is identified as the E2 component of pyruvate dehydrogenase complex (PDC-E2) [1,2]. Many studies in patients and animal models have demonstrated that the interplay of genetics and the environment with the innate and adaptive immune systems is highly orchestrated in the pathogenesis of PBC. Of note, CD8 T cells play a critical role in biliary destruction [1–3].

The bile duct is configured by biliary epithelial cells (BECs, also known as cholangiocytes) and comprises a finely organized biliary network. BECs participate in bile secretion and bile acid reabsorption. Additionally, BECs provide the first line of defense against microbes in the biliary system through several immunological pathways, including various pathogen pattern recognition receptors [4]. By TdT-mediated deoxyuridine triphosphate nick-end labeling (TUNEL) staining of liver sections of humans, previous studies demonstrated that increased apoptosis of BECs was observed in patients with PBC compared with normal controls and other chronic cholestatic diseases such as primary sclerosing cholangitis, with similar degrees of inflammation [5–7]. Furthermore, PDC-E2, the autoantigen of PBC, is shown to localize in the apoptotic bodies where it is accessible to be recognized by AMAs [8,9]. Hence, apoptosis of BECs is speculated as the initial step of tolerance breakdown in PBC. However, these observations are from samples in patients with advanced diseases. It is unclear whether apoptosis of BECs occurs in the induction stage of PBC.

Gut microbiota plays several crucial roles in the host's health. A diverse and balanced microbial community is required to typically develop the innate and adaptive immune system [10]. Compositional and functional alterations of the gut microbiome, called dysbiosis, can cause immune dysregulation and lead to inflammatory disorders [11].

Abbreviations: 2-OA, 2-octynoic acid; 2-OA-OVA, 2-octynoic acid conjugated ovalbumin; AMAs, anti-mitochondrial antibodies; AIC, autoimmune cholangitis; BECs, biliary epithelial cells; PBC, primary biliary cholangitis; PDC-E2, E2 component of pyruvate dehydrogenase complex; TLR, toll-like receptor; TUNEL, TdT-mediated deoxyuridine triphosphate nick-end labeling.

* Corresponding author. Department of Clinical Laboratory Sciences and Medical Biotechnology, College of Medicine, National Taiwan University, No. 1, Chang-Te Street, 100229, Taipei, Taiwan.
E-mail address: yahuichuang@ntu.edu.tw (Y.-H. Chuang).

https://doi.org/10.1016/j.jtauto.2022.100182
Received 15 December 2022; Accepted 20 December 2022
Available online 21 December 2022

Dysbiosis is an essential factor in the pathogenesis of many autoimmune diseases, such as inflammatory bowel disease and rheumatoid arthritis, and liver diseases, such as alcoholic liver disease, nonalcoholic fatty liver disease, and liver cirrhosis [12,13]. Of note, reduced species richness and a significant shift in the overall microbial diversity are observed in patients with PBC [14,15]. These observations suggest that gut microbiota affects hepatic immune balance in PBC.

The early immunological events leading to PBC are poorly studied since clinical signs of disease occur late in the pathological process, and early samples are difficult to get. In this study, we took advantage of our 2-OA-OVA-induced mouse model of autoimmune cholangitis (AIC) to study the initiation of PBC. 2-octynoic acid (2-OA), a xenobiotic (compounds foreign to a living organism), is mimic of the highly conserved inner lipoyl domain of PDC-E2 autoantigen [16]. Mice immunized with 2-OA-OVA (2-OA coupled with ovalbumin) and α-galactosylceramide (α-GalCer) develop high titer of AMAs, and autoimmune cholangitis with a significant increase in lymphocyte infiltrates, portal inflammation, granuloma formation, bile duct damage, and, in particular, fibrosis [17,18]. We reported that apoptotic BECs and gut dysbiosis was notable in the early stage of murine AIC. BECs in AIC mice expressed adhesion molecules, cytokines/chemokines, and toll-like receptors (TLRs). Moreover, BECs treated with TLR2 ligand had elevated apoptosis and CXCL10 production. Our results highlight that apoptotic BECs and gut dysbiosis occur in the early stage and lead to the onset of PBC.

2. Materials and methods

2.1. Preparation of 2-OA-OVA

2-OA (500 mg, Alfa Aesar, Haverhill, MA, USA) and *N*-hydroxysuccinimide (NHS, 410.9 mg) in dry 1, 4-dioxane (10 mL) were stirred for 20 min under nitrogen. Then *N, N′*-dicyclohexylcarbodiimide (DCC, 736.6 mg) was quickly added while opening into the mixture to avoid water vapor in the reaction and stirred overnight to form 2-OA-NHS. 2-OA-NHS was filtered and concentrated by rotavaporation under reduced pressure. The mixture was dissolved with ethyl ether (5 mL), washed with brine, and dried under magnesium sulfate. The mixture was filtered, and the filtrate was concentrated and then purified using flash chromatography (silica gel; ethyl acetate/hexane 2:3) to give NHS-activated 2-OA. NHS-activated 2-OA (636 mg) was dissolved in dimethyl sulfoxide (DMSO) (3670 mL) and mixed with OVA (2180 mg, 0.1 M sodium bicarbonate buffer) in a shaker at room temperature for 3 h 2-OA-OVA in the supernatant was dialyzed using a dialysis tube (cut-off 8000 Da) against ddH_2O and then lyophilized for storing.

2.2. Xenobiotic 2-OA-OVA-induced autoimmune cholangitis mouse model

Male and female C57BL/6 mice, aged 7–9 weeks, were immunized with 20 μg 2-OA-OVA in the presence of complete Freund's adjuvant (CFA, Sigma–Aldrich, St. Louis, MO, USA) and boosted with 2-OA-OVA in incomplete Freund's adjuvant (IFA, Sigma-Aldrich) two weeks later using intraperitoneal injection. Two μg of α-galactosylceramide (KRN7000, Cayman Chemical, Ann Arbor, MI, USA) were administered with the first 2-OA-OVA immunization by intravenous injection. All mice were purchased from the National Laboratory Animal Center, Taiwan, and housed under specific-pathogen-free (SPF) conditions with a 12:12 light-dark cycle at the Laboratory Animal Center of National Taiwan University College of Medicine. The Institutional Animal Care and Use Committee (IACUC) of the National Taiwan University College of Medicine approved the mouse care and handling procedures.

2.3. Detection of serum anti-PDC-E2 IgG by ELISA

ELISA plates were coated with 5 μg/mL recombinant PDC-E2 diluted with carbonate buffer (pH 9.6) at 4 °C overnight and were blocked with 1% casein (Sigma-Aldrich) for 1 h at room temperature. Diluted sera were added for 2 h at room temperature. After washing, HRP-labeled anti-mouse IgM and IgG (1:2000, Invitrogen, Camarillo, CA, USA) were added for detection. The tetramethylbenzidine (TMB) substrate (Clinical Science Products, Mansfield, MA, USA) was added to each well for 15 min and stopped with 1 N H_2SO_4. The absorbance was read on a SpectraMax® M2 Microplate Reader (Molecular Devices, San Jose, CA, USA) at 450 and 540 nm.

Table 1
List of primers for quantitative RT-PCR.

β-actin	Forward: CACAGTGTTGTCTGGTGGTA
	Reverse: GACTCATCGTACTCCTGCTT
TNF-α	Forward: CCCCAAAGGGATGAGAAGTTC
	Reverse: TGAGGGTCTGGGCCATAGAA
IFN-γ	Forward: GGCCATCAGCAACAACATAAGC
	Reverse: TGGACCACTCGGATGAGCTCA
TLR2	Forward: CAGCTTAAAGGGCGGGTCAGAG
	Reverse: TGGAGACGCCAGCTCTGGCTCA
TLR3	Forward: GGGGTCCAACTGGAGAACCT
	Reverse: CCGGGGAGAACTCTTTAAGTGG
TLR4	Forward: GCCTTTCAGGGAATTAAGCTCC
	Reverse: AGATCAACCGATGGACGTGTA
TLR5	Forward: CACTCCCTCGGAGAACCCA
	Reverse: GGCCTTGAAAAACATCCCAAC
TLR7	Forward: TCTTACCCTTACCATCAACCACA
	Reverse: CCCCAGTAGAACAGGTACACA
TLR9	Forward: ACTGAGCACCCCTGCTTCTA
	Reverse: AGATTAGTCAGCGGCAGGAA

2.4. Liver mononuclear cell quantitation

The livers were perfused with phosphate-buffered saline containing 0.2% BSA and dissociated with the gentleMACS™ Dissociator (Miltenyi Biotec, Auburn, CA, USA). The parenchymal cells were removed as pellets after centrifugation at 50×*g* for 5 min, and the non-parenchymal cells were isolated using 40% and 70% Percoll (GE HealthCare Biosciences, Quebec, Canada). Subsets of liver mononuclear cells were obtained using flow cytometry. Cells were incubated with anti-CD16/32 (clone 93, Biolegend, San Diego, CA, USA) at room temperature for 10 min before staining with fluorochrome-conjugated monoclonal antibodies (mAb) against cell surface markers, including CD3 (clone 145-2C11), CD4 (clone GK1.5), CD8a (clone 53–6.7), NK1.1 (clone PK136), and CD19 (clone 6D5) (Biolegend, San Diego, CA, USA) at 4 °C for 30 min. Stained cells were measured using a flow cytometer (BD FACSVerse) and analyzed using FlowJo software (Tree Star, Ashland, OR, USA).

2.5. Isolation of bile ducts

The liver was perfused with Hank's Balanced Salt Solution (HBSS) without calcium, magnesium, and phenol red (Gibco, Thermo Scientific, Wilmington, DE, USA) containing 5 mM EGTA (Sigma Aldrich) at a rate of 8 mL/min for 5 min, then perfused with HBSS containing 0.05% type IV collagenase (Gibco) and 5 mM $CaCl_2$ (Sigma Aldrich) for 5–8 min. The liver was collected, and the biliary tree was obtained after removing the hepatic parenchyma with a soft interdental brush. Intrahepatic small bile ducts in the peripheral region of the biliary tree were collected. Tissue samples were snap-frozen in liquid nitrogen and stored at −80 °C.

2.6. RT-qPCR

Total RNA from the liver, proximal colon, or isolated bile duct was obtained using TRI^{zol} (Invitrogen Life Technologies, Carlsbad, CA, USA). cDNA was synthesized using High-Capacity cDNA Reverse Transcription Kits (Applied Biosystems, Foster City, CA, USA), followed by real-time PCR (SYBR green; Applied Biosystems) with an ABI 7500 Fast Real-Time PCR system (Applied Biosystems). Primers were designed according to the published sequences and listed in Table 1 β-actin served as

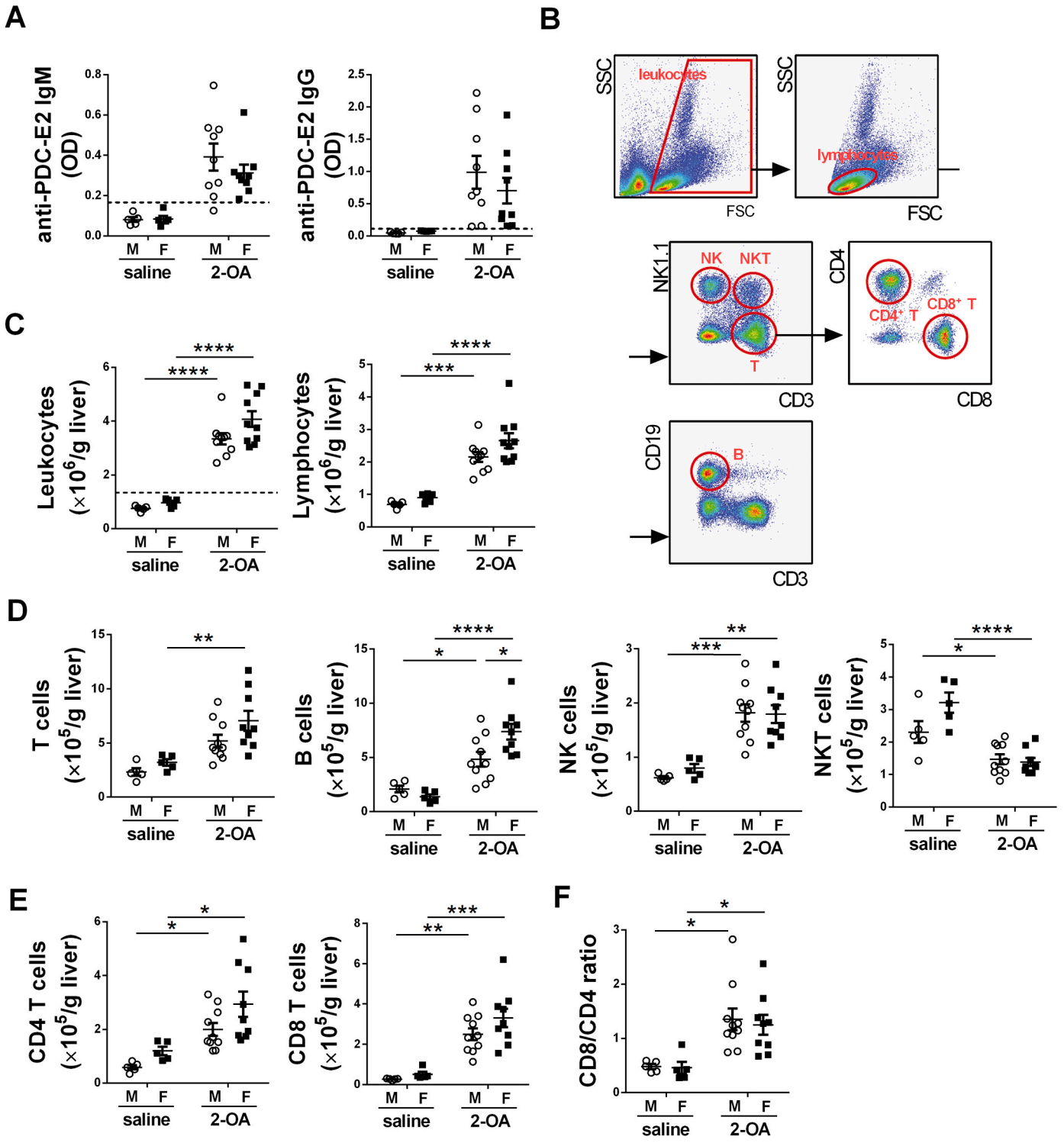

Fig. 1. Both male and female mice immunized with 2-OA-OVA developed AMAs and liver inflammation. Male and female mice were immunized with 2-OA-OVA or normal saline, and serum levels of AMAs and liver lymphocytes were examined at 3 weeks post-immunization. (A) Serum levels of anti-PDC-E2 IgM and IgG were determined using ELISA. OD, optical density. (B) Representative flow plots show the gating strategies of different subsets of cells. (C) Liver leukocytes and lymphocytes were quantified. (D) The numbers of T, B, NK, and NKT cells in the liver were quantified. (E) The numbers of CD4 T and CD8 T cells in the liver were quantified. (F) The ratio of CD8/CD4 was calculated. M, male mice; F, female mice. The dashed lines in (A) and (C) depict the cut-off for a positive response, calculated as the mean of the results of saline-treated samples plus three standard deviations. Symbols represent one individual mouse, and bars indicate mean ± SEM. n = 5–10 mice per group. *, $p < 0.05$; **, $p < 0.01$; ***, $p < 0.001$; ****, $p < 0.0001$ (two-way ANOVA followed by Tukey's multiple comparison test).

an internal control. Expression levels of mRNA were calculated as $2^{-\Delta\Delta CT}$

2.7. Stool sample collection and fecal DNA extraction

Two hundred mg of fecal specimens were collected in a sterile 2 mL centrifuge tube, snap-frozen in liquid nitrogen, and stored at −80 °C

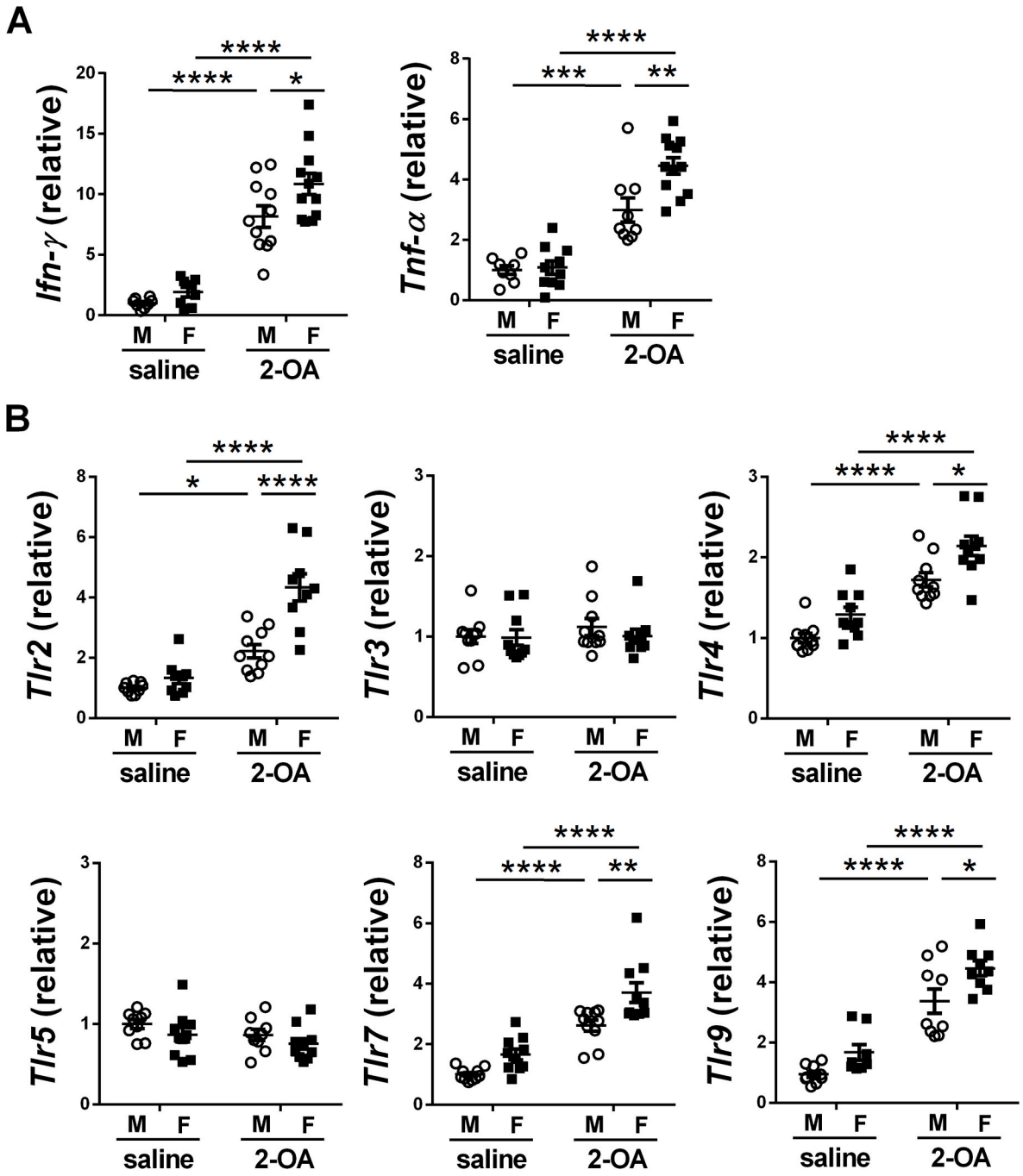

Fig. 2. Increased expression of liver pro-inflammatory cytokines and TLRs in AIC mice. Male and female mice were immunized with 2-OA-OVA or normal saline and examined at 3 weeks post-immunization. The expression levels of (A) IFN-γ and TNF-α and (B) TLRs in the liver were detected using RT-qPCR. M, male mice; F, female mice. Symbols represent one individual mouse, and bars indicate mean ± SEM. n = 8–12 mice per group. *, $p < 0.05$; **, $p < 0.01$; ***, $p < 0.001$; ****, $p < 0.0001$ (two-way ANOVA followed by Tukey's multiple comparison test).

until DNA extraction. Bacterial DNA in these specimens was isolated via a QIAamp Fast DNA Stool Mini Kit (Qiagen, Hilden, Germany) following the user's guide. Extracted DNA was dissolved in 50 μL ddH2O, and the purity and quality of the DNA were assessed by a Nanodrop 1000 spectrophotometer (Thermo Scientific, Wilmington, DE, USA).

2.8. NGS of bacterial 16S-rRNA genes

The v3 and v4 regions of bacterial 16s rRNA gene were amplified using 5′-TCG TCG GCA GCG TCA GAT GTG TAT AAG AGA CAG CCT ACG GGN GGC WGC AG-3′ and 5′-GTC TCG TGG GCT CGG AG A TGT GTA TAA GAG ACA GGA CTA CGV GGG TAT CTA ATC C-3′ as forward and reverse primers and 2X KAPA HiFi HotStart ReadyMix (KAPA Biosystems, Woburn, MA, USA). These polymerase chain reaction (PCR) products, the size of 550 base pairs, were subjected to PCR clean-up using AMPure XP beads (Beckman Coulter Genomics, Danvers, MA, USA). A subsequent second PCR involving the above amplicons was conducted to incorporate dual indices and Illumina sequencing adapters using a Nextera XT Index Kit (Illumina, San Diego, CA, USA). AMPure XP beads were again applied to clean up the PCR products, and the resulting amplicons were sequenced on an Illumina MiSeq System (Illumina) according to the manufacturer's standard protocol.

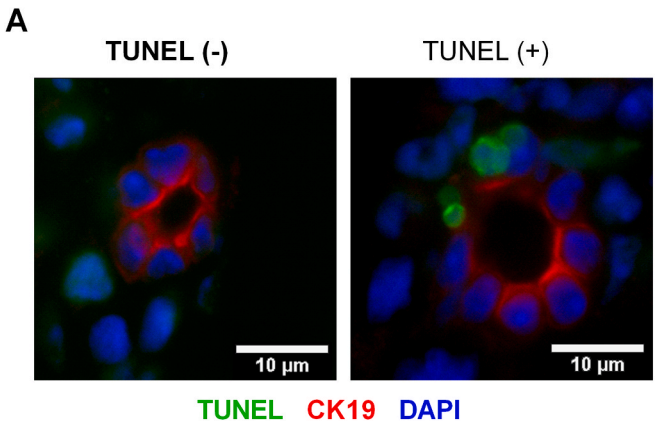

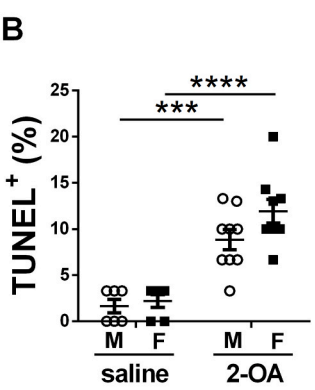

Fig. 3. Apoptosis of BECs in AIC mice. Male and female mice were immunized with 2-OA-OVA or normal saline. Three weeks post-immunization, apoptosis of BECs in the liver tissues of mice was measured by TUNEL assay. (A) Representative images of TUNEL assay of liver histopathology (1000× magnification, scale bar, 10 μm). The liver section was triple labeled for apoptotic cells (green), biliary cytokeratin CK-19 (red), and nuclei DAPI (blue). (B) Thirty intrahepatic small bile ducts were counted in each slide to calculate the frequency of bile ducts with TUNEL-positive cells. M, male mice; F, female mice. Symbols represent one individual mouse, and bars indicate mean ± SEM. n = 6–9 mice per group. ***, $p < 0.001$; ****, $p < 0.0001$ (two-way ANOVA followed by Tukey's multiple comparison test).

2.9. Immunofluorescence assay and TUNEL assay

Portions of liver tissue were trimmed and fixed with 4% paraformaldehyde solution (Santa Cruz Biotechnology, Dallas, TX, USA) immediately for 5 min under room temperature and, after that, incubated in 6% sucrose in PBS for 1 h, 12% sucrose for 1 h, 18% sucrose for 2 h, and 24% sucrose overnight at 4 °C. Tissue was immersed in Tissue-Tek® O·C.T. Compound (Sakura Finetek, Torrance, CA, USA) and sliced into the 5-μm section. The frozen tissue sections were fixed with 4% paraformaldehyde solution for 10 min at room temperature, blocked with 3% BSA for 60 min at room temperature, permeabilized with 0.3% Triton-x solution for 10 min at room temperature, and then incubated with primary antibodies, anti-cytokeratin 19 (ab52625, 500x dilution, Abcam, Cambridge, UK) and anti-MHC class II (ab25333, 150x dilution, Abcam) overnight at 4 °C. After four PBST (0.2%) washing, incubation with a cocktail containing Alexa488-conjugated secondary antibody (ab150157, 500x dilution, Abcam), Alexa594-conjugated secondary antibody (ab150080, 500x dilution, Abcam) and DAPI (4′,6-diamidino-2-phenylindole dihydrochloride, D8417, Sigma-Aldrich) was performed for 60 min at room temperature in the dark and ultimately mounted with mounting medium (Bio-Rad Laboratories, Inc., Hercules, CA, USA). For apoptotic cells detection, the sections were stained using ApopTag® Fluorescein *in Situ* Apoptosis Detection Kit (Merck Millipore, Billerica, MA, USA) before being post-fixed in pre-cooled ethanol-acetic acid. Images were taken with an Olympus IX83 fluorescence microscope (Olympus, Tokyo, Japan).

2.10. In vitro apoptosis assay

603B cells, a non-tumorigenic mouse cholangiocyte cell line, were seeded in each well of a 6-well plate (1×10^5/well) and treated with Pam3CSK4 (5 μg/mL, Invivogen, San Diego, CA, USA) in the presence of TNF-α (100 ng/mL, PeproTech, Cranbury, NJ, USA) and SC-514 (50 nM, Cayman Chemical) for 24 h [19]. Cells were then stained with Annexin V and 7-AAD to detect apoptosis. Stained cells were measured using a 2-laser CytoFLEX flow cytometer (Beckman Coulter) and analyzed using FlowJo software (Tree Star, Ashland, OR, USA). The percentages of Annexin $V^+7\text{-}AAD^-$ (early apoptosis) and annexin V^+ $7\text{-}AAD^+$ (late apoptosis) were counted as apoptotic cells.

2.11. Statistical analysis

Data are expressed as the mean ± standard error of the mean (SEM). Statistical analysis was determined by two-way ANOVA followed by Tukey's multiple comparison test (Figs. 1–6) or two-sided paired Student's t-test (Fig. 7). Statistically significant differences were defined as p values of less than 0.05 (Prism 6; Graph-Pad Software, La Jolla, CA, USA).

3. Results

3.1. Mice immunized with xenobiotics induce autoantibodies and liver inflammation

2-OA, a xenobiotic, is widely found in the environment, including perfumes, lipstick, and many accepted food flavorings [16]. Hence, the female predominance of PBC may be because they contact more 2-OA than males. To investigate the role of environmental xenobiotics in the pathogenesis of PBC, we exposed male and female littermate mice to equivalent 2-OA-OVA to induce AIC and detected their anti-PEC-E2 autoantibodies and liver inflammation at 3 weeks post-immunization. As shown in Fig. 1, both male and female mice immunized with 2-OA-OVA had elevated serum levels of anti-PDC-E2 antibodies (Fig. 1A) and infiltrated immune cells in the liver (Fig. 1B and C). Moreover, all female mice immunized with 2-OA-OVA were considered positive in autoantibody levels and immune cells (Fig. 1A and C). Lymphocytes, including CD4 and CD8 T, B, and NK cells, were increased in both male AIC and female AIC mice, while NKT cells were decreased (Fig. 1D and E). Although both CD4 T cells and CD8 T cells were increased in 2-OA-OVA immunization, there were more increases in CD8 T cells than in CD4 T cells (Fig. 1F). The expression levels of pro-inflammatory cytokines, IFN-γ and TNF-α, in the liver were increased in male AIC mice and female AIC mice (Fig. 2A). Levels of Toll-like receptor (TLR) 2, 4, 7, and 9 in the liver had marked increases in male AIC mice and female AIC mice (Fig. 2B). Notably, significantly higher levels of IFN-γ, TNF-α, TLR2, 4, 7, and 9 were found in female AIC mice than in male AIC mice (Fig. 2). The results highlighted the importance of environmental triggers in the development of AIC. However, female mice developed higher AIC than males may be because of their immune responses triggered by xenobiotic exposure.

3.2. Apoptosis and cytokines/chemokines production of BECs in AIC mice

To investigate whether apoptosis of BECs occurred in the disease's early stage, we examined the apoptosis of BECs in AIC mice at 3 weeks post-immunization. As shown in Fig. 3, there were more apoptotic BECs ($TUNEL^+$ $CK19^+$) in AIC mice than in control mice. We further investigated whether BECs act as antigen-presenting cells by detecting the expression of MHC II molecules on BEC using immunofluorescence staining of liver tissues. There were no positive signals of IA^b in $CK19^+$

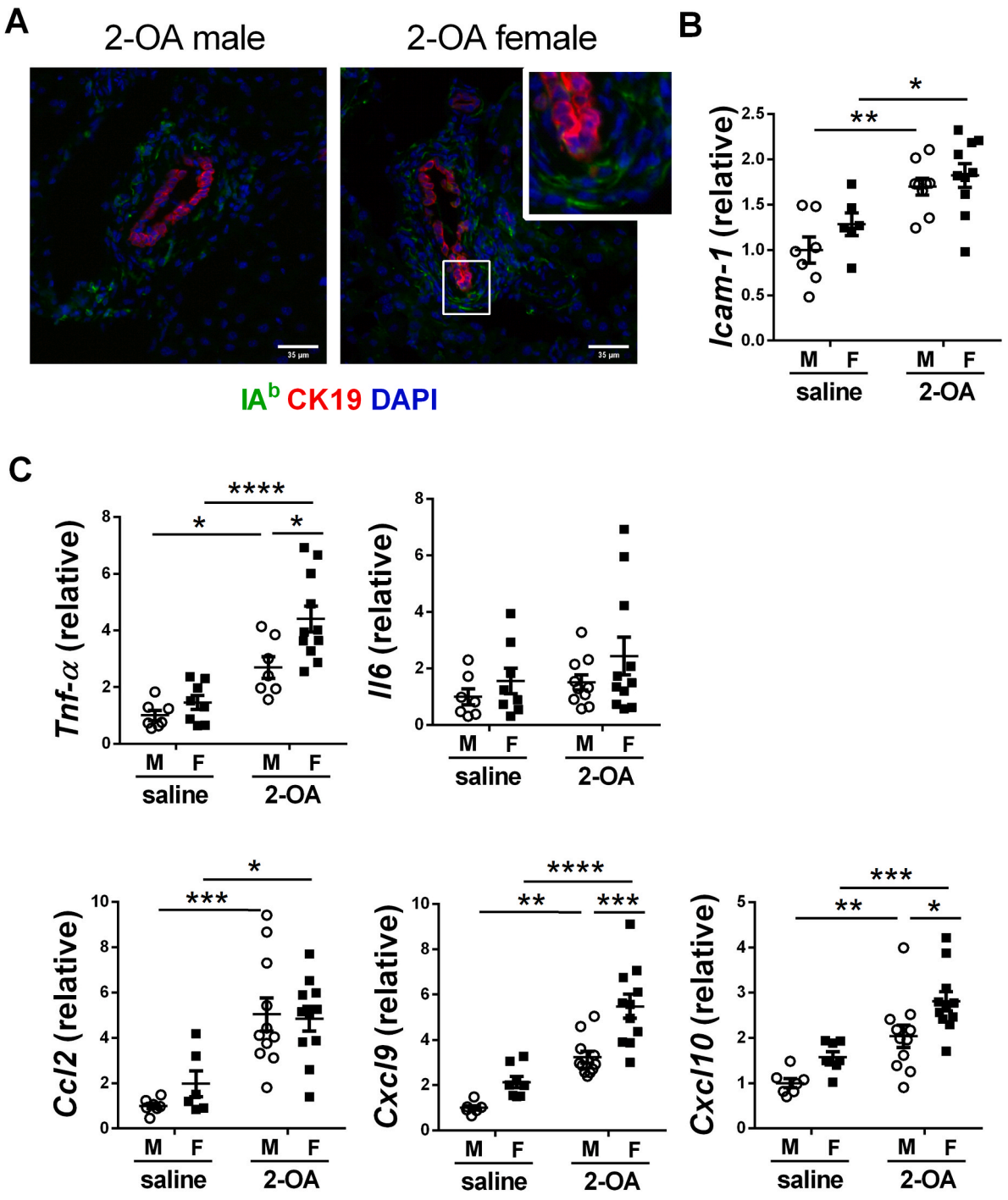

Fig. 4. Adhesion molecules and cytokines/chemokines of BECs in AIC mice. Male and female mice were immunized with 2-OA-OVA or normal saline. Three weeks post-immunization, liver tissues, and intrahepatic small bile ducts were taken. (A) Representative images of MHC class II (IAb) expression in liver histopathology (400× magnification, scale bar, 35 μm). The liver section was triple labeled for IA^b (green), biliary cytokeratin CK-19 (red), and nuclei DAPI (blue). (B) The expression levels of ICAM-1 mRNA in the intrahepatic small bile duct were detected by RT-qPCR. (C) The expression levels of TNF-α, IL-6, CCL2, CXCL9, and CXCL10 mRNA in the intrahepatic small bile duct were detected by RT-qPCR. M, male mice; F, female mice. Symbols represent one individual mouse, and bars indicate mean ± SEM. n = 6–11 mice per group. *, $p < 0.05$; **, $p < 0.01$; ***, $p < 0.001$; ****, $p < 0.0001$ (two-way ANOVA followed by Tukey's multiple comparison test).

BECs of male AIC mice and female AIC mice. Cells expressed IA^b were around the bile duct (Fig. 4A). Increased expression levels of adhesion molecule ICAM-1 in bile ducts were observed in AIC mice compared with saline-treated controls (Fig. 4B). Expression levels of inflammatory cytokines/chemokines TNF-α, CCL-2, CXCL9, and CXCL10 in the bile duct were also increased in AIC mice. In addition, the expression levels of TNF-α, CCL-2, CXCL9, and CXCL10 were markedly higher in female AIC mice than in male AIC mice. However, the levels of IL-6 in bile ducts were not different among the four groups (Fig. 4C).

3.3. Altered compositions of gut microbiota of mice after 2-OA-OVA immunization

TLRs expressed on sentinel cells, such as macrophages and dendritic cells, and non-immune cells can recognize various microbial components and mediate the immune responses [20]. Due to increased levels of

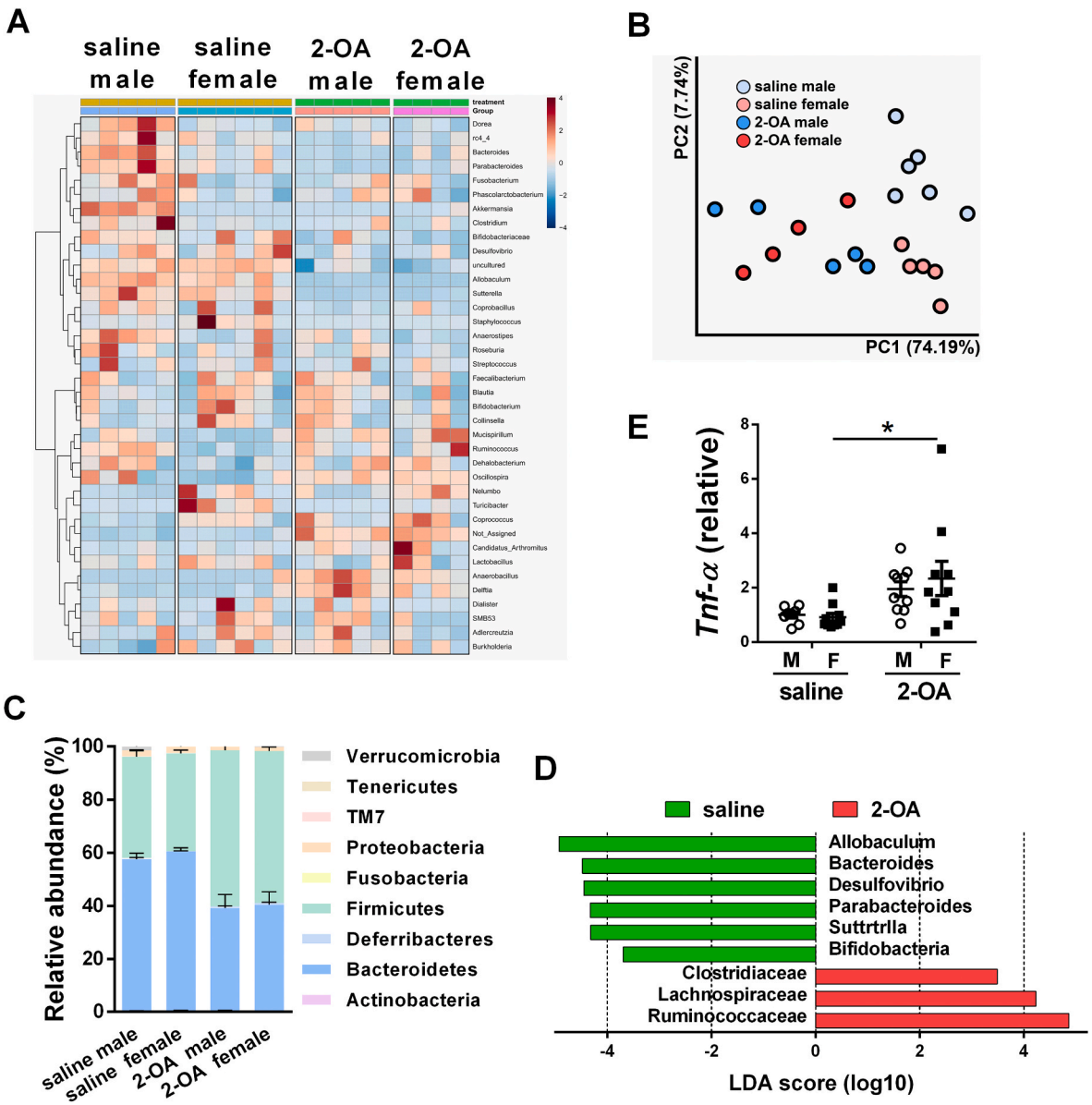

Fig. 5. Marked alternation of gut microbiota after 2-OA-OVA immunization. Male and female mice were immunized with 2-OA-OVA or normal saline. Fecal samples of mice were collected at 3 weeks post-immunization. Gut microbiota compositions were profiled by 16s rRNA next-generation sequencing (NGS). (A) Hierarchical clustering heat map of microbiota abundance at the genus level. Highly relative abundance bacteria were in red. Lowly relative abundance bacteria were in blue. (B) Microbial communities were analyzed by principal coordinate analysis (PCoA) based on the weighted UniFrac distance metric. (C) Relative abundance of fecal microbiota at the phylum level of the taxonomy. (D) Histograms of linear discriminant analysis (LDA) effect size (LEfSe) comparison between fecal microbiota at the family level. Only the taxa having an LDA >3.0 were shown. Log-level changes in LDA scores were displayed on the x-axis. Green bars: taxa found in greater relative abundance in saline controls. Red bars: taxa found in greater relative abundance in 2-OA-OVA immunization. (E) The expression levels of TNF-α mRNA in the intestines were detected by RT-qPCR. Symbols represent one individual mouse, and bars indicate mean ± SEM. n = 6–11 mice per group. *, $p < 0.05$ (two-way ANOVA followed by Tukey's multiple comparison test).

TLR in the liver of AIC mice, we then investigated whether and how gut microbiota affects the liver. We analyzed fecal microbiota compositions of AIC mice through high-throughput 16S ribosomal RNA gene amplicon sequencing. The heat map depicted relative bacterial abundance at the genus level among four groups of mice (Fig. 5A). PCoA plots with weighted UniFrac matrices showed a clear separation of microbial communities in AIC mice and control mice (Fig. 5B). Fecal microbiota in four groups of mice at the phylum level was dominated by *Firmicutes* and *Bacteroidetes* (>90%), followed by *Verrucomicrobia* (<3%), *Proteobacteria* (<3%), *Actinobacteria* (<1%), and *Deferribacteres* (<1%). Notably, normal saline-treated mice had higher Bacteroidetes over Firmicutes, while 2-OA-OVA-immunized mice were the opposite (Fig. 5C). Linear discrimination analysis effect size (LEfSe) analysis highlighted that *Clostridiaceae*, *Lachnospiraceae*, and *Ruminococcaceae* were enriched in AIC mice (Fig. 5D). In addition, increased expression levels of TNF-α in the intestine were noted in AIC mice (Fig. 5E).

3.4. TLR2 signaling induced apoptosis of BEC

We proposed that dysbiotic gut microbiota leads to apoptosis of BECs via microbial cell components interacting with TLR on BEC. We detected expression levels of TLRs in the bile duct of AIC mice and found levels of TLR2, 7, and 9 in bile ducts had marked increases in AIC mice. Notably, higher expression of TLR2 was noted in female AIC mice than in male AIC mice (Fig. 6). To clarify whether TLR2 signaling induced apoptosis of BEC, we treated 603B cells (a non-tumorigenic mouse cholangiocyte

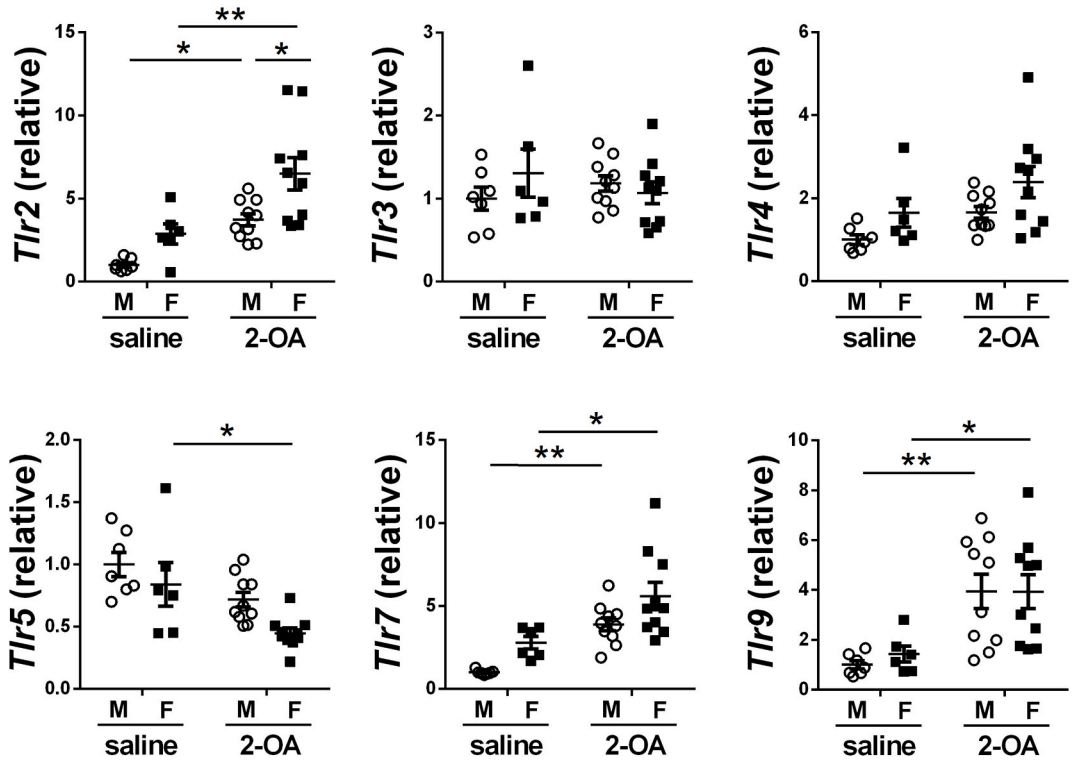

Fig. 6. Expression of TLRs of the intrahepatic small bile duct in AIC mice. Male and female mice were immunized with 2-OA-OVA or normal saline. The expression levels of TLRs mRNA in the intrahepatic small bile duct of mice at 3 weeks post-immunization were detected by RT-qPCR. M, male mice; F, female mice. Symbols represent one individual mouse, and bars indicate mean ± SEM. n = 6–10 mice per group. *, $p < 0.05$; **, $p < 0.01$ (two-way ANOVA followed by Tukey's multiple comparison test).

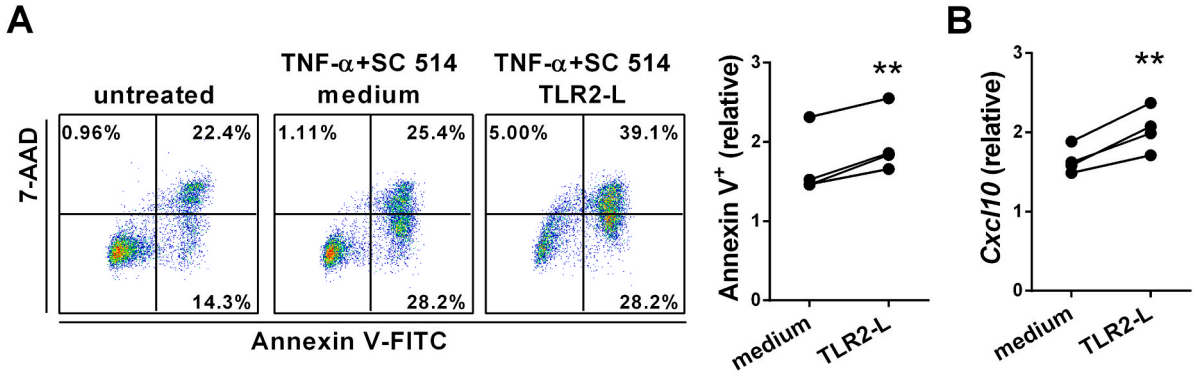

Fig. 7. Increased apoptosis of TLR2 ligand-stimulated BEC. 603B cells were stimulated with Pam3CSK4 (TLR2 ligand) or not in the presence of TNF-α and SC-514 for 24 h. (A) Representative and graphical summary of flow cytometry analysis of apoptosis of 603B cells. (B) The expression levels of CXCL10 mRNA in treated 603B cells were detected by RT-qPCR. Data were normalized based on 603B cells without stimulation (untreated). Individual symbols represent an independent experiment. **, $p < 0.01$ (two-tailed paired *t*-test).

cell line) with Pam3CSK4 (TLR2 ligand) for 24 h and detected their apoptosis. As shown in Fig. 7A, there was an elevated frequency of apoptotic 603B cells when treated with TLR2 ligand in the presence of TNF-α and NF-kB inhibitor SC-514 compared to cells treated with TNF-α and SC-514. Moreover, there were higher expression levels of CXCL10 in 603B cells treated with TLR2 ligand than in controls (Fig. 7B).

4. Discussion

In this study, we took advantage of our 2-OA-OVA-induced mouse model to study the initiation of PBC. Our results showed that the altered composition of gut microbiota, in particular, increased Gram-positive *Firmicutes* in AIC mice was observed when they were examined only 3 weeks after immunization. In addition, apparent apoptosis of BECs in AIC mice was also noted. BECs expressed the adhesion molecule ICAM-1 and secreted chemoattractant cytokines and chemokines. Several TLRs, mainly TLR2, were highly expressed in the bile duct of AIC mice. Moreover, BECs treated with the TLR2 ligand had elevated apoptosis and CXCL10 production.

We and others show that the xenobiotic 2-OA is an essential trigger in PBC because 2-OA can modify cellular proteins to form neoantigens and induce tolerance breakdown of PBC by molecular mimicry [16–18,21]. In addition, we found that 2-OA can cause altered gut microbiota with an increased *Firmicutes/Bacteroidetes* (F/B) ratio in this study. Accumulating evidence indicates that many xenobiotics, such as heavy metals, pesticides, antibiotics, and food additives, are metabolized by the gut

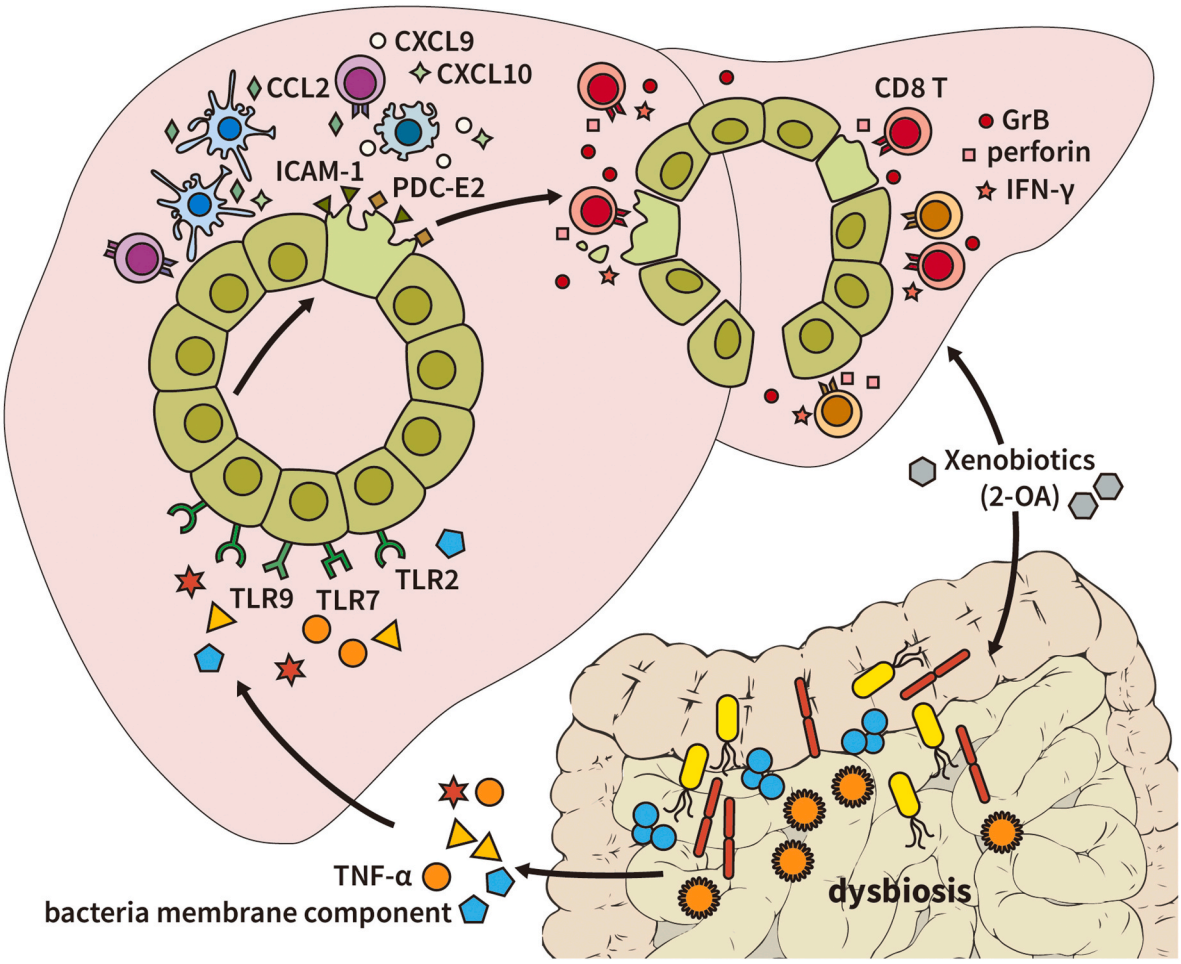

Fig. 8. Overall schema of the initiation of PBC. Exposure to environmental xenobiotics alters gut microbiota composition and induces intestinal inflammation. Gut microbiota membrane components and TNF-α induces apoptosis of BECs, which leads to autoantigen release. Injured BECs express more adhesion molecules ICAM-1 and chemoattractants CCL2, CXCL9, and CXCL10 to recruit immune cells. Among infiltrated immune cells in the portal area, CD8 T cells are responsible for further biliary destruction by secreting more IFN-γ and cytotoxic molecules perforin and granzyme B.

microbiome and can profoundly perturb the composition and function of the gut microbiota to affect host health status [22]. For example, antibiotic vancomycin can reduce microbial diversity, decrease gram-positive bacteria, and cause a compensatory increase in gram-negative bacteria [23]. The artificial sweetener saccharin enhances the risk of glucose intolerance by inducing dysbiosis and altering microbial metabolic pathways [24]. In addition, consistent with our finding, chronic lead exposure perturbs gut microbiota with decreased *Bacteroidetes* and increased *Firmicutes* [25]. The gram-positive *Firmicutes* and gram-negative *Bacteroidetes* are the most common bacteria in the gut microbiota of humans and mice. The *Firmicutes/Bacteroidetes* (F/B) ratio is associated with maintaining homeostasis, and changes in this ratio can lead to various diseases [26]. Microbial membrane components such as lipopolysaccharides of gram-negative *Bacteroidetes* and peptidoglycan and lipoteichoic acid of gram-positive *Firmicutes* can regulate the host immune response through TLR4/MD2 and TLR2 signaling, respectively [27].

Apoptosis of BECs is speculated as the initial step of tolerance breakdown in PBC [5–9]. In this study, apoptosis of BECs could be observed in liver sections at an early stage of 2-OA-OVA-induced AIC mice. In addition, elevated expression of TNF-α in the liver, bile duct, and intestine of AIC mice was also noted. Previous studies and our *in vitro* stimulation experiment show that TNF-α is one of the critical inflammatory modulators that can induce apoptosis in BECs [28,29]. Moreover, BECs could express multiple TLRs to promote appropriate activation of the innate immune system against exogenous pathogens and mediate the fine interaction between the host and its intestinal microflora [20,30–32]. This study showed a higher expression of TLRs in the liver tissue and intrahepatic small bile ducts of AIC mice, and BEC treated with the TLR2 ligand had elevated apoptosis. These results suggest that TNF-α induces apoptosis of BEC and the binding of the microbial products of gut microbiota to TLR2 in BEC enhances apoptosis of BEC.

We found that BECs in AIC mice expressed the ICAM-1 and secreted CCL2, CXCL9, and CXCL10. These results are consistent with previous studies that ICAM-1, an essential molecule for lymphocyte adhesion, is strongly expressed in the bile duct of patients with PBC [33,34], and BECs derived from patients with PBC stimulated with pro-inflammatory cytokines could express HLA I, HLA II, and adhesion molecule ICAM-1 and secrete cytokines and chemokines [34,35]. However, MHC II expression on BECs of our model mice was undetectable. CCL2, CXCL9, and CXCL10 are important chemotactic agents for the recruitment of immune cells, such as monocytes and T cells in PBC [36]. These results suggest an essential involvement of BECs in the recruitment of circulating leukocytes that can migrate to the portal area.

Our previous study showed markedly elevated functional effector CD8 T cells with increased IFN-γ, perforin, or granzyme B expression in AIC mice (unpublished data). In this study, adhesion molecules ICAM-1 and CD8 T cell-chemoattractants CCL2, CXCL9, and CXCL10 in the bile duct of AIC mice were increased. By histopathological assessment of liver samples of human PBC, a previous study showed that $CD8^+$ T cells could enter into BECs, and the entry of CD8 T cells in BECs is correlated

with TUNEL-positive BECs [37]. These results suggest that CD8 T cells are recruited to the bile duct and induce apoptosis of BECs by releasing effector molecules.

5. Conclusions

Our results suggest a new mechanism for the breakdown of tolerance in PBC. Exposure to environmental xenobiotics alters gut microbiota composition and induces intestinal inflammation. Gut microbiota membrane components and TNF-α induces apoptosis of BECs, which leads to autoantigen release. Injured BECs express more adhesion molecule ICAM-1 and chemoattractants CCL2, CXCL9, and CXCL10 to recruit immune cells. Among infiltrated immune cells in the portal area, CD8 T cells are responsible for further biliary destruction by secreting more IFN-γ and cytotoxic molecules perforin and granzyme B (Fig. 8).

Financial Support

This work was supported by grants from the National Health Research Institutes, Taiwan (NHRI-EX110-11028SI, NHRI-EX111-11028SI, NHRI-EX112-11028SI).

Author contributions

Conceptualization, Y.-H. C.; Methodology, Y.-W. W., C.-I. L., H.-W. C., and J.-C. W.; Validation, Y.-W. W., C.-I. L., H.-W. C., J.-C. W. and Y.-H. C.; Investigation, Y.-W. W., C.-I. L., H.-W. C., J.-C. W. and Y.-H. C.; Writing – Original Draft, Y.-W. W., and Y.-H. C.; Writing – Review & Editing, Y.-H. C.; Funding Acquisition, Y.-H. C.; Supervision, Y.-H. C.

Declaration of competing interest

The authors declare that they have no known competing financial interests or personal relationships that could have appeared to influence the work reported in this paper.

Data availability

Data will be made available on request.

Acknowledgments

We like to acknowledge the service provided by the Medical Microbiota Center of the First Core Laboratory at National Taiwan University College of Medicine and the Flow Cytometric Analyzing and Sorting Core Facility at National Taiwan University Hospital.

References

[1] U. Beuers, M.E. Gershwin, R.G. Gish, P. Invernizzi, D.E. Jones, K. Lindor, et al., Changing nomenclature for PBC: from 'cirrhosis' to 'cholangitis, Hepatology 62 (2015) 1620–1622.
[2] A. Lleo, P.S.C. Leung, G.M. Hirschfield, E.M. Gershwin, The pathogenesis of primary biliary cholangitis: a comprehensive Review, Semin. Liver Dis. 40 (2020) 34–48.
[3] T. Katsumi, K. Tomita, P.S. Leung, G.X. Yang, M.E. Gershwin, Y. Ueno, Animal models of primary biliary cirrhosis, Clin. Rev. Allergy Immunol. 48 (2015) 142–153.
[4] Y.H. Chuang, R.Y. Lan, M.E. Gershwin, The immunopathology of human biliary cell epithelium, Semin. Immunopathol. 31 (2009) 323–331.
[5] K. Harada, S. Ozaki, M.E. Gershwin, Y. Nakanuma, Enhanced apoptosis relates to bile duct loss in primary biliary cirrhosis, Hepatology 26 (1997) 1399–1405.
[6] K. Harada, S. Furubo, S. Ozaki, K. Hiramatsu, Y. Sudo, Y. Nakanuma, Increased expression of WAF1 in intrahepatic bile ducts in primary biliary cirrhosis relates to apoptosis, J. Hepatol. 34 (2001) 500–506.
[7] J. Tinmouth, M. Lee, I.R. Wanless, F.W. Tsui, R. Inman, E.J. Heathcote, Apoptosis of biliary epithelial cells in primary biliary cirrhosis and primary sclerosing cholangitis, Liver 22 (2002) 228–234.
[8] A. Lleo, C. Selmi, P. Invernizzi, M. Podda, R.L. Coppel, I.R. Mackay, et al., Apotopes and the biliary specificity of primary biliary cirrhosis, Hepatology 49 (2009) 871–879.
[9] A. Lleo, C.L. Bowlus, G.X. Yang, P. Invernizzi, M. Podda, J. Van de Water, et al., Biliary apotopes and anti-mitochondrial antibodies activate innate immune responses in primary biliary cirrhosis, Hepatology 52 (2010) 987–998.
[10] M.B. Geuking, Y. Koller, S. Rupp, K.D. McCoy, The interplay between the gut microbiota and the immune system, Gut Microb. 5 (2014) 411–418.
[11] M. Levy, A.A. Kolodziejczyk, C.A. Thaiss, E. Elinav, Dysbiosis and the immune system, Nat. Rev. Immunol. 17 (2017) 219–232.
[12] J. Henao-Mejia, E. Elinav, C.A. Thaiss, P. Licona-Limon, R.A. Flavell, Role of the intestinal microbiome in liver disease, J. Autoimmun. 46 (2013) 66–73.
[13] L.A. Yurkovetskiy, J.M. Pickard, A.V. Chervonsky, Microbiota and autoimmunity: exploring new avenues, Cell Host Microbe 17 (2015) 548–552.
[14] R. Tang, Y. Wei, Y. Li, W. Chen, H. Chen, Q. Wang, et al., Gut microbial profile is altered in primary biliary cholangitis and partially restored after UDCA therapy, Gut 67 (2018) 534–541.
[15] M. Furukawa, K. Moriya, J. Nakayama, T. Inoue, R. Momoda, H. Kawaratani, et al., Gut dysbiosis associated with clinical prognosis of patients with primary biliary cholangitis, Hepatol. Res. 50 (2020) 840–852.
[16] K. Amano, P.S. Leung, R. Rieger, C. Quan, X. Wang, J. Marik, et al., Chemical xenobiotics and mitochondrial autoantigens in primary biliary cirrhosis: identification of antibodies against a common environmental, cosmetic, and food additive, 2-octynoic acid, J. Immunol. 174 (2005) 5874–5883.
[17] S.J. Wu, Y.H. Yang, K. Tsuneyama, P.S. Leung, P. Illarionov, M.E. Gershwin, et al., Innate immunity and primary biliary cirrhosis: activated invariant natural killer T cells exacerbate murine autoimmune cholangitis and fibrosis, Hepatology 53 (2011) 915–925.
[18] Y.H. Hsueh, Y.N. Chang, C.E. Loh, M.E. Gershwin, Y.H. Chuang, AAV-IL-22 modifies liver chemokine activity and ameliorates portal inflammation in murine autoimmune cholangitis, J. Autoimmun. 66 (2016) 89–97.
[19] J. Liu, A.N. Eischeid, X.M. Chen, Col1A1 production and apoptotic resistance in TGF-beta1-induced epithelial-to-mesenchymal transition-like phenotype of 603B cells, PLoS One 7 (2012), e51371.
[20] F.A. Carvalho, J.D. Aitken, M. Vijay-Kumar, A.T. Gewirtz, Toll-like receptor-gut microbiota interactions: perturb at your own risk, Annu. Rev. Physiol. 74 (2012) 177–198.
[21] L. Wang, F.S. Wang, C. Chang, M.E. Gershwin, Breach of tolerance: primary biliary cirrhosis, Semin. Liver Dis. 34 (2014) 297–317.
[22] C.F. Maurice, H.J. Haiser, P.J. Turnbaugh, Xenobiotics shape the physiology and gene expression of the active human gut microbiome, Cell 152 (2013) 39–50.
[23] A. Vrieze, C. Out, S. Fuentes, L. Jonker, I. Reuling, R.S. Kootte, et al., Impact of oral vancomycin on gut microbiota, bile acid metabolism, and insulin sensitivity, J. Hepatol. 60 (2014) 824–831.
[24] J. Suez, T. Korem, D. Zeevi, G. Zilberman-Schapira, C.A. Thaiss, O. Maza, et al., Artificial sweeteners induce glucose intolerance by altering the gut microbiota, Nature 514 (2014) 181–186.
[25] J. Xia, C. Jin, Z. Pan, L. Sun, Z. Fu, Y. Jin, Chronic exposure to low concentrations of lead induces metabolic disorder and dysbiosis of the gut microbiota in mice, Sci. Total Environ. 631–632 (2018) 439–448.
[26] P.J. Turnbaugh, R.E. Ley, M.A. Mahowald, V. Magrini, E.R. Mardis, J.I. Gordon, An obesity-associated gut microbiome with increased capacity for energy harvest, Nature 444 (2006) 1027–1031.
[27] O. Takeuchi, K. Hoshino, T. Kawai, H. Sanjo, H. Takada, T. Ogawa, et al., Differential roles of TLR2 and TLR4 in recognition of gram-negative and gram-positive bacterial cell wall components, Immunity 11 (1999) 443–451.
[28] P. Shivakumar, T. Mizuochi, R. Mourya, S. Gutta, L. Yang, Z. Luo, et al., Preferential TNFalpha signaling via TNFR2 regulates epithelial injury and duct obstruction in experimental biliary atresia, JCI Insight 2 (2017), e88747.
[29] G. Alpini, Y. Ueno, L. Tadlock, S.S. Glaser, G. LeSage, H. Francis, et al., Increased susceptibility of cholangiocytes to tumor necrosis factor-alpha cytotoxicity after bile duct ligation, Am. J. Physiol. Cell Physiol. 285 (2003) C183–C194.
[30] K. Harada, S. Ohira, K. Isse, S. Ozaki, Y. Zen, Y. Sato, et al., Lipopolysaccharide activates nuclear factor-kappaB through toll-like receptors and related molecules in cultured biliary epithelial cells, Lab. Invest. 83 (2003) 1657–1667.
[31] M. Nakamura, K. Funami, A. Komori, T. Yokoyama, Y. Aiba, A. Araki, et al., Increased expression of Toll-like receptor 3 in intrahepatic biliary epithelial cells at sites of ductular reaction in diseased livers, Hepatol Int 2 (2008) 222–230.
[32] K. Harada, K. Isse, Y. Nakanuma, Interferon gamma accelerates NF-kappaB activation of biliary epithelial cells induced by Toll-like receptor and ligand interaction, J. Clin. Pathol. 59 (2006) 184–190.
[33] D.H. Adams, S.G. Hubscher, J. Shaw, G.D. Johnson, C. Babbs, R. Rothlein, et al., Increased expression of intercellular adhesion molecule 1 on bile ducts in primary biliary cirrhosis and primary sclerosing cholangitis, Hepatology 14 (1991) 426–431.
[34] R.C. Ayres, J.M. Neuberger, J. Shaw, R. Joplin, D.H. Adams, Intercellular adhesion molecule-1 and MHC antigens on human intrahepatic bile duct cells: effect of pro-inflammatory cytokines, Gut 34 (1993) 1245–1249.
[35] C.M. Morland, J. Fear, G. McNab, R. Joplin, D.H. Adams, Promotion of leukocyte transendothelial cell migration by chemokines derived from human biliary epithelial cells in vitro, Proc. Assoc. Am. Phys. 109 (1997) 372–382.
[36] A.T. Borchers, S. Shimoda, C. Bowlus, C.L. Keen, M.E. Gershwin, Lymphocyte recruitment and homing to the liver in primary biliary cirrhosis and primary sclerosing cholangitis, Semin. Immunopathol. 31 (2009) 309–322.
[37] S.X. Zhao, W.C. Li, N. Fu, G.D. Zhou, S.H. Liu, L.N. Jiang, et al., Emperipolesis mediated by CD8(+) T cells correlates with biliary epithelia cell injury in primary biliary cholangitis, J. Cell Mol. Med. 24 (2020) 1268–1275.